

Target Localization Techniques and Tools for MIMO Radar

Hana Godrich[°], Alexander M. Haimovich[°], and Rick S. Blum[†]

[°]New Jersey Institute of Technology, Newark, NJ 07102

[†]Lehigh University, Bethlehem, PA 18015-3084

[°][hg44,haimovich]@njit.edu, [†]rblum@eecs.lehigh.edu

Abstract—MIMO (multiple-input multiple-output) radar refers to an architecture that employs multiple, spatially distributed transmitters and receivers. The widely spaced antenna structure suggests unique features that set MIMO radar apart from other radar systems, making it strongly related to MIMO communications. The widely separated transmit/receive antennas capture different aspects of the target cross section that can be exploited to obtain diversity gain for detection and estimation of the target's various parameters, such as angle of arrival, and Doppler. The use of coherent processing can provide localization accuracy gains well beyond that supported by the radar's waveform. This paper provides a review of some recent work on computing the Cramer-Rao lower bound (CRLB) on the achievable localization accuracy. The geometric dilution of precision (GDOP) is used as a tool for assessing and illustrating the localization accuracy of the Best Linear Unbiased Estimator (BLUE).

Index Terms—MIMO radar, spatial processing, adaptive array.

I. INTRODUCTION

MIMO radar is defined broadly as a radar system employing multiple transmit waveforms and having the ability to jointly process signals received at multiple receive antennas. Elements of MIMO radar transmit independent waveforms resulting in an omnidirectional beampattern or create diverse beampatterns by controlling correlations among transmitted waveforms [1], [2]. MIMO radar may be configured with its antennas colocated or widely distributed over an area. MIMO radar is an emerging concept, but it is already apparent that it has the potential to make important contributions to the radar field. In [3] it is observed that MIMO radar has more degrees of freedom than systems with a single transmit antenna. These additional degrees of freedom support flexible time-energy management modes [4], lead to improved angular resolution [5], [6], and improve parameter identifiability [7]. With widely separated antennas, MIMO radar has the ability to improve radar performance by exploiting radar cross section (RCS) diversity [8], handle slow moving targets by exploiting Doppler estimates from multiple directions [9], and support high accuracy target localization [10].

From a model point of view, widely separated antennas take advantage of the spatial properties of extended targets, while with colocated antennas; the target is modeled as a point

with no spatial properties. Each configuration and model has its strengths and challenges. With colocated antennas, MIMO radars can mimic beamformers utilizing low probability of intercept (LPI) waveforms. Rather than focusing energy on a target, the transmitted energy is evenly distributed in space [11]. The loss of processing gain compared to conventional phased array beamforming due to the uniform illumination is compensated by the gain in time, since a narrow beam does not need to be scanned as in a phased array [12]. MIMO spatial signatures in systems with colocated antennas can be exploited to estimate radar parameters (location, RCS) of multiple targets, but the ability to resolve targets is limited by the Rayleigh resolution limit of the transmit/receive arrays. Widely separated antennas support high accuracy target localization, and by focusing on the effect of the channel, create a link between MIMO radar and MIMO communications.

MIMO systems have led to a revolution in wireless communications [13]. Recent publications (for example, [14], [15], and references therein) indicate that one can exploit similar ideas in radar, suggesting interesting cross-fertilization of ideas between MIMO communications and MIMO radar. For quite some time, it has been understood that radar targets provide a rich scattering environment yielding 5 to 20 dB target RCS fluctuations. Such targets display essentially independent scattering returns when radiated from sufficiently different directions [16]. The premise of MIMO radar with widely separated antennas is that angular spread (RCS variations as a function of aspect) can be exploited to improve radar performance in a variety of ways. The parallel to MIMO communication is recognized in the similar roles that the transmission medium (channel) and target play in respectively, communication and radar. In other words, the target serves as the "channel" in the radar problem. For example, combining target returns resulting from independent illuminations yields a diversity gain akin to the diversity gain obtained in the communication problem over fading channels when the data is transmitted through independent channels. Diversity gains are well understood in communications [17]. In radar, the idea is that any individual look at the target might have a small amplitude return with a significant probability, but by increasing the number of looks, the probability that all the looks have small amplitude returns can be made arbitrarily small. Diversity gain is only one of two key gains that MIMO communications can provide. The other gain is called spatial multiplexing [13]. Spatial multiplexing in MIMO communications expresses the ability to use transmit

A. M. Haimovich work was supported by the U.S. Air Force Office of Scientific Research, Agreement FA9550-06-1-0026. R. S. Blum work was supported by the Air Force Research Laboratory under agreement No. FA9550-06-1-0041

and receive antennas to set up a multidimensional space for signaling. Similarly, in MIMO radar, a multidimensional signal space is created when the returns from multiple scatterers or targets combine to generate a rich backscatter. With proper design, transmit-receive paths can be separated and exploited for improving radar performance.

In this tutorial paper, we review features of MIMO radar with coherent processing for target localization. The distinction between non-coherent and coherent applications relies on the need for merely time synchronization between the transmitting and receiving radars vs. the need for phase synchronization. As the potential for localization performance enhancement is evident from the ambiguity function [10], the lower bound on the attainable accuracy is set by developing the Cramer-Rao lower bound in section III. The bound is shown to be proportional to the carrier wavelength squared, and independent of the signal bandwidth, for narrow band signals. Two target localization estimators are presented in IV: the maximum likelihood estimator (MLE) and the best linear unbiased estimator (BLUE). The last provides an insight into the relation between sensors locations, target location, and localization accuracy. To establish a more comprehensive expression of these relations, a metric widely used in Global Positioning Systems (GPS) for mapping estimation precision and known as geometric dilution of precision (GDOP) is introduced in section V.

II. SYSTEM MODEL

The MIMO radar scheme is based on a system with M transmitting radars and N receiving radars, widely distributed. It is assumed to be both time and phase synchronized. The transmitting and receiving radars are located in a two dimensional plane (x, y) . Considering a point target located at coordinates $X = (x, y)$, where the reflectivity of the target is spatially homogeneous and is modeled by the complex value $\zeta = \zeta_{re} + j\zeta_{im}$. Let the target be illuminated by the M transmitters arbitrarily located at coordinates $T_k = (x_{tk}, y_{tk})$, $k = 1, \dots, M$. The signals scattered by the target are collected by N sensors placed at arbitrary coordinates $R_\ell = (x_{r\ell}, y_{r\ell})$, $\ell = 1, \dots, N$. The set of transmitted waveforms in low-pass equivalent form is $\sqrt{E_e} s_k(t)$, $k = 1, \dots, M$, where $\int_{\mathcal{T}} |s_k(t)|^2 dt = 1$, the normalized transmitted energy is $E_e = E/M$, while E is the total transmitted energy, and \mathcal{T} is the waveforms' duration. Let all transmitted waveforms have the same bandwidth W . Further specification of the waveforms $s_k(t)$ depends on the application. A set of orthogonal waveform is transmitted, where orthogonality is assumed to be maintained such that $\int_{\mathcal{T}} s_k(t) s_m^*(t - \tau) dt = 0$ for all $k \neq m$, and for all time delays of interest. Path loss effects are neglected, i.e., the model accounts for the effect of the sensors/target localizations only through time delays (or phase shifts) of the signals.

It can be easily shown that the lowpass equivalent of the signal observed at sensor ℓ reflected by a scatterer at coordinates $X = (x, y)$ is given by:

$$r_\ell(t) = \sqrt{E_e} \sum_{k=1}^M h_{\ell k} s_k(t - \tau_{\ell k}) + w_\ell(t), \quad (1)$$

where $h_{\ell k} = \zeta \exp(-j2\pi f_c \tau_{\ell k})$, the total signal time delay is $\tau_{\ell k} = \tau_{tk} + \tau_{r\ell}$, the propagation time delay between the k -th transmitting sensor located at coordinates T_k and the target at X is $\tau_{tk} = \frac{1}{c} \sqrt{(x_{tk} - x)^2 + (y_{tk} - y)^2}$ and the propagation time from the target to the ℓ -th receiving sensor is $\tau_{r\ell} = \frac{1}{c} \sqrt{(x_{r\ell} - x)^2 + (y_{r\ell} - y)^2}$, the carrier frequency is denoted by f_c , the speed of light by c , and $w_\ell(t)$ is a circularly symmetric, zero-mean, complex Gaussian noise, spatially and temporally white with autocorrelation function $\sigma_w^2 \delta(\tau)$.

The received signal at each sensor is a mixture of the transmitted signals reflected by the target. The mixture of signals is separated at the receiver end by exploiting the orthogonality between the transmitted waveforms.

III. CRLB ON TARGET LOCALIZATION ESTIMATION

The ambiguity function concept has long been used in the context of localization [18]. In [10] it has been used to provide a comparative performance of coherent vs. non-coherent processing of MIMO radar waveforms. The high accuracy localization benefits of coherent MIMO radar systems are inherent in the ambiguity function plots. To set the lower bound on the attainable accuracy in the coherent case, the CRLB needs to be derived.

The CRLB provides a lower bound for the mean square error (MSE) of any unbiased estimator for an unknown parameter(s). Given a vector parameter $\boldsymbol{\theta} = [x, y, \zeta_{re}, \zeta_{im}]^T$, its unbiased estimate $\hat{\boldsymbol{\theta}} = [\hat{x}, \hat{y}, \hat{\zeta}_{re}, \hat{\zeta}_{im}]^T$ satisfies the following inequality [19]:

$$E_{\boldsymbol{\theta}} \left\{ \left(\hat{\boldsymbol{\theta}}_i - \boldsymbol{\theta}_i \right) \left(\hat{\boldsymbol{\theta}}_i - \boldsymbol{\theta}_i \right)^T \right\} \geq [\mathbf{J}^{-1}(\boldsymbol{\theta})]_{i,i}, \quad (2)$$

where $\mathbf{J}(\boldsymbol{\theta})$ is the Fisher Information matrix (FIM) given by:

$$\mathbf{J}(\boldsymbol{\theta}) \stackrel{\text{def}}{=} E_{\boldsymbol{\theta}} \left\{ \frac{\partial}{\partial \boldsymbol{\theta}} \log p(\mathbf{r}|\boldsymbol{\theta}) \left(\frac{\partial}{\partial \boldsymbol{\theta}} \log p(\mathbf{r}|\boldsymbol{\theta}) \right)^T \right\}, \quad (3)$$

For the signal model in (1), the joint probability density function (pdf) of the observations (time samples at multiple receive antennas) $p(\mathbf{r}; \boldsymbol{\theta})$ parameterized by the unknown parameters vector $\boldsymbol{\theta}$, is then:

$$p(\mathbf{r}; \boldsymbol{\theta}) \propto \exp \left\{ -\frac{1}{\sigma_w^2} \sum_{\ell=1}^N \int_{\mathcal{T}} \left| r_\ell(t) - \sqrt{E_e} \sum_{k=1}^M h_{\ell k} s_k(t - \tau_{\ell k}(X)) \right|^2 dt \right\}. \quad (4)$$

Let the CRLB matrix be defined as:

$$\mathbf{C}_{CRLB} = [\mathbf{J}(\boldsymbol{\theta})]^{-1}. \quad (5)$$

While the CRLB expresses the minimum mean-square error (MMSE) of the estimate of $\boldsymbol{\theta} = [x, y, \zeta_{re}, \zeta_{im}]^T$, we are really interested only in the estimation of x and y . The target reflectivity terms ζ_{re} and ζ_{im} serve as nuisance parameters. For the variances of the estimates of x and y , it is sufficient

to derive the submatrix $[\mathbf{C}_{CRLB}]_{2 \times 2} = [\mathbf{J}(\boldsymbol{\theta})]_{2 \times 2}^{-1}$, denoting the first 2x2 submatrix of $[\mathbf{J}(\boldsymbol{\theta})]^{-1}$. The diagonal elements of the $[\mathbf{C}_{CRLB}]_{2 \times 2}$ submatrix provide the information for the MMSE $\sigma_x^2 \geq [\mathbf{C}_{CRLB}]_{1,1}$ and $\sigma_y^2 \geq [\mathbf{C}_{CRLB}]_{2,2}$.

In [20] the CRLB submatrix for the target position estimates, in the coherent case, is shown to be:

$$[\mathbf{C}_{CRLB}]_{2 \times 2} = \left(\mathbf{H} \boldsymbol{\Lambda}_{\mathbf{x}_c} \mathbf{H}^T - \mathbf{V} \mathbf{H} \boldsymbol{\Lambda}_{\zeta}^{-1} \mathbf{H}^T \mathbf{V}^T \right)^{-1}, \quad (6)$$

where the following notations are being used:

$$\boldsymbol{\Lambda}_{\mathbf{x}_c} = 8\pi^2 SNR (f_c^2 + \beta^2) \mathbf{I}_{NM \times NM}, \quad (7)$$

$$\boldsymbol{\Lambda}_{\zeta} = SNR \frac{MN}{|\zeta|^2} \mathbf{I}_{2 \times 2},$$

$$\mathbf{V} = \frac{4\pi f_c SNR}{|\zeta|^2} \begin{bmatrix} -\zeta_{im} & \zeta_{re} \\ \vdots & \vdots \\ -\zeta_{im} & \zeta_{re} \end{bmatrix}_{NM \times 2},$$

$$\mathbf{H} = \begin{bmatrix} A_{11} & \dots & A_{MN} \\ B_{11} & \dots & B_{MN} \end{bmatrix}_{MN \times MN},$$

where SNR is the signal-to-noise ratio term, defined as $SNR = E_e / |\zeta|^2$, and the term β is the effective bandwidth defined as $\beta = \frac{\int_W f^2 |S(f)|^2 df}{\int_W |S(f)|^2 df}$, where the integration is over the bandwidth W . The rows of matrix \mathbf{H} are defined by the terms $A_{\ell k} = \cos \phi_{tk} + \cos \phi_{r\ell}$ and $B_{\ell k} = \sin \phi_{tk} + \sin \phi_{r\ell}$, such that $\phi_{tk} = \tan^{-1} \left(\frac{y - y_{tk}}{x - x_{tk}} \right)$ and $\phi_{r\ell} = \tan^{-1} \left(\frac{y - y_{r\ell}}{x - x_{r\ell}} \right)$ are the phases created by the geometric information of the radars location configuration relative to the target position.

The MMSE for the target position for the x axis is

$$\sigma_x^2 (MMSE) = \frac{c^2}{8\pi^2 SNR f_c^2 f_R} \cdot \frac{g_{xc}}{u_{CRLB_c}} \quad (8)$$

and for the y axis is

$$\sigma_y^2 (MMSE) = \frac{c^2}{8\pi^2 SNR f_c^2 f_R} \cdot \frac{g_{yc}}{u_{CRLB_c}} \quad (9)$$

where f_R is a the ratio $f_R = \left(1 + \frac{\beta^2}{f_c^2} \right)$ and the terms u_{CRLB_c} , g_{xc} and g_{yc} relate to the geometric layout of the transmitting and receiving radars compared with the target location, as follows:

$$g_{xc} = \left[\text{sum} (B_{\ell k}^2) - \frac{(\text{sum} (B_{\ell k}))^2}{f_R MN} \right], \quad (10)$$

for the x axis coefficient, where the following notation is used

$$\text{sum}(\circ) = \sum_{k=1}^M \sum_{\ell=1}^N (\circ).$$

The y axis coefficient g_{yc} :

$$g_{yc} = \left[\text{sum} (A_{\ell k}^2) - \frac{(\text{sum} (A_{\ell k}))^2}{f_R MN} \right], \quad (11)$$

and the common term u_{CRLB_c} is:

$$u_{CRLB_c} = [g_{xc}] \cdot [g_{yc}] - \left[\text{sum} (A_{\ell k} B_{\ell k}) - \frac{\text{sum} (A_{\ell k}) \text{sum} (B_{\ell k})}{f_R MN} \right]^2. \quad (12)$$

These terms are summations of the terms $A_{\ell k}$ and $B_{\ell k}$ that represent the geometric relation between the sensors locations and the target location.

The expressions for the MMSEs for target location estimate given in (8) and (9) can provide some insight into the performance of coherent MIMO radars, as follows:

- The MMSEs expressions show that the achievable accuracy is inversely proportional to $f_c^2 (1 + \frac{\beta^2}{f_c^2})$, due to the use of the phase information across different paths. For narrow band signals, where $\frac{\beta}{f_c} \ll 1$, and therefore, $f_R \approx 1$, the localization accuracy is inversely proportional to the carrier frequency f_c^2 and independent of the effective bandwidth. It is apparent that coherent processing offers an accuracy gain when compared with the effective bandwidth, for narrow band signals.

- The MMSEs terms are strongly reliant on the geographical spread of the radar systems, compared with the target location. This dependency is integrated into the terms $\frac{g_{xc}}{u_{CRLB_c}}$ and $\frac{g_{yc}}{u_{CRLB_c}}$. From these terms one cannot intuitively identify the relation between the radars positions and the obtainable accuracy. For this reason, we need to define a more suitable method to express these relations. The GDOP metric provides these tools.

- The CRLB is known to provide a good bound in high SNR. As for low SNR, the CRLB does not give a rigorous bound. As the time estimates are based on matched filters at the receiver end, the ambiguity features of the signal waveforms predominate the estimation capabilities in low SNR conditions. A more rigid bound needs to be found for the localization error variance in the low SNR case.

IV. TARGET LOCATION ESTIMATION

Once an expression for the lower bound on the MSE for target localization has been provided, target localization techniques can be evaluated. Two estimators are presented: the maximum likelihood estimator (MLE) and the best linear unbiased estimator (BLUE). The MLE is motivated by its asymptotic optimality, while the BLUE by its closed form expression.

A. Target Localization using MLE

The MLE is a practical estimator in the sense that its application to a problem of observations in white Gaussian noise is relatively straightforward. Moreover, under mild conditions on the probability density function of the observations, the MLE of the unknown parameters is asymptotically unbiased, and it asymptotically attains the CRLB [19].

For the case of MIMO radar, the signal waveform received by radar ℓ is given in (1). The MLE of the unknown parameter vector $\boldsymbol{\theta} = [x, y, \zeta_{re}, \zeta_{im}]^T$ given the observation vector \mathbf{r} is given by [19]:

$$\begin{aligned} \hat{\boldsymbol{\theta}}_{ML} &= \arg \left\{ \max_{\boldsymbol{\theta}} [\log p(\mathbf{r}; \boldsymbol{\theta})] \right\} \\ &= \arg \left\{ \max_{\mathbf{x}} \left\{ \max_{\zeta_{re}, \zeta_{im}} [\log p(\mathbf{r}; \mathbf{x}, \zeta_{re}, \zeta_{im})] \right\} \right\}, \end{aligned} \quad (13)$$

where \mathbf{x} defines the location vector $\mathbf{x} = [x, y]^T$, and $p(\mathbf{r}; \theta)$ was expressed in (4). We are not interested in estimating ζ_{re} , ζ_{im} explicitly, but this is needed for the estimation of x and y . Recall that $\zeta_{re} + j\zeta_{im} = \zeta$, hence the MLE of ζ is found from the following condition on the log-likelihood:

$$\frac{\partial}{\partial \zeta} \log p(\mathbf{r}; \mathbf{x}, \zeta) \Big|_{\zeta=\hat{\zeta}_{ML}} = 0. \quad (14)$$

Using (4) in (14) the MLE for the reactivity index is derived in [10] and substituted back into (13). The MLE for \mathbf{x} is then given by maximizing the log-likelihood function $\log p(\mathbf{r}; \mathbf{x} | \hat{\zeta}_{ML})$ with respect to \mathbf{x} such that [10]:

$$\hat{\mathbf{x}}_{MLE} = \arg \left\{ \max_{\mathbf{x}} \left[\sum_{k=1}^M \sum_{\ell=1}^N \rho_{lk} \int r_{\ell}(t) s_k^*(t - \tau_{\ell k}(\mathbf{x})) dt \right] \right\}, \quad (15)$$

where $\rho_{lk} = \exp(j2\pi f_c \tau_{\ell k})$. Since a closed form expression can not be found for the MLE in (15), numerical methods need to be applied. A grid search or an iterative maximization of the likelihood function needs to be performed to determine $\hat{\mathbf{x}}_{MLE}$. This might involve a significant computational effort. In practice, we can limit the search grid for high resolution target localization estimation to an area around a preliminary non-coherent location estimate $X_c = (x_c, y_c)$. When iteration methods are used to determine $\hat{\mathbf{x}}_{MLE}$, this estimate can serve to initialize the search.

B. Target Localization using BLUE

The MLE derived in Section (IV-A) does not have a closed form expression, and numerical methods need to be used to solve it. A different approach to the localization problem is by using a linear perturbation model of the target location and use of the BLUE. This estimator provides a closed form solution, and enables a comprehensive evaluation of the performance.

To develop the BLUE, a linear perturbation model needs to be defined for the relation between the signals time delays and the target location. To do so, we start with the propagation time estimate of a signal transmitted by the k -th transmitting radar located at coordinates $T_k = (x_{tk}, y_{tk})$, reflected by a target located at $X = (x, y)$ and received by a radar located at $R_l = (x_{rl}, y_{rl})$ that can be approximated as :

$$\hat{\tau}_{lk} = \tau_{lk} + \varepsilon_{lk}, \quad \forall k = 1, \dots, M, l = 1, \dots, N, \quad (16)$$

where τ_{lk} , the propagation time, is the sum of the time delays from radar k to the target and from the target to radar l :

$$\tau_{lk} = \frac{\sqrt{(x_{tk} - x)^2 + (y_{tk} - y)^2}}{c} + \frac{\sqrt{(x_{rl} - x)^2 + (y_{rl} - y)^2}}{c}, \quad (17)$$

and ε_{lk} is the estimation error.

As we can see in (17), the relation between the time delay and the target's coordinates is nonlinear. In order to express the time delays τ_{lk} as a linear function of perturbations of the x and y coordinates measured relative to an arbitrary point $X_c = (x_c, y_c)$. The perturbed point X_c can be obtained by an

initial, nominal estimation. Using notation defined previously, the time delay between a transmitter-receiver pair is given by using the Taylor series expansion of τ_{lk} around (x_c, y_c) , resulting in a linear perturbation model for the time delay, as a function of the displacements x and y from perturbed point X_c , as follows [21]:

$$\tau_{lk} \approx -\frac{x}{c} (\cos \phi_{tk}^c + \cos \phi_{r\ell}^c) - \frac{y}{c} (\sin \phi_{tk}^c + \sin \phi_{r\ell}^c), \quad (18)$$

where the angles ϕ_{tk}^c and $\phi_{r\ell}^c$ are the angles that the transmitting radar k and receiving radar ℓ , respectively, create with the reference axis $X_c = (x_c, y_c)$. Letting $A_{lk}^c = \cos \phi_{tk}^c + \cos \phi_{r\ell}^c$ and $B_{lk}^c = \sin \phi_{tk}^c + \sin \phi_{r\ell}^c$, we can express the time delays in the following simplified form:

$$\tau_{lk} \approx -\frac{x}{c} A_{lk}^c - \frac{y}{c} B_{lk}^c. \quad (19)$$

The linear relation between vector $\boldsymbol{\tau} = [\tau_{11}, \tau_{12}, \dots, \tau_{NM}]^T$ and the vector of unknowns $\boldsymbol{\varphi} = [x, y, \mu]^T$, where the set (x, y) stands for the target position and μ is an unknown nuisance parameter produced by the time-offset between the radars and the target, can be written as follows:

$$\boldsymbol{\tau} = \mathbf{D}\boldsymbol{\varphi}, \quad (20)$$

where the angle dependent matrix \mathbf{D} is defined as:

$$\mathbf{D} = -\frac{1}{c} \begin{bmatrix} A_{11}^c & B_{11}^c & 1 \\ \dots & \dots & \dots \\ A_{NM}^c & B_{NM}^c & 1 \end{bmatrix}_{NM \times 3}. \quad (21)$$

We postulate the following model between the observable time delays and the target location

$$\hat{\boldsymbol{\tau}} = \mathbf{D}\boldsymbol{\varphi} + \boldsymbol{\varepsilon}, \quad (22)$$

where $\boldsymbol{\varepsilon} = [\varepsilon_{11}, \varepsilon_{12}, \dots, \varepsilon_{NM}]^T$ is the $MN \times 1$ measurement noise vector. Notice that one of the differences between the MLE and BLUE models is that the MLE target localization is carried out utilizing signal observations, while according to (22), the BLUE's "observations" are in the form of time delays. So an intermediate step of time delay estimation is implied. The time delays estimates used as observations τ_{lk} are derived by the MLE as follows:

$$\tau_{lk} = \arg \max_v \left[\exp[j2\pi f_c v] \int r_{\ell}(t) s_k^*(t - v) dt \right], \quad (23)$$

where v is a dummy variable for the time delay. It is shown in [21] that the maximum likelihood time delay estimates are unbiased with error covariance matrix

$$\mathbf{C}_{\boldsymbol{\varepsilon}} = \frac{\sigma_w^2}{8\pi^2 \text{SNR} f_c^2 f_R} \mathbf{I}_{NM \times NM}. \quad (24)$$

For the linear and Gaussian model in (22), the BLUE is computed from the Gauss-Markov theorem [19] that states the BLUE of the unknown vector $\boldsymbol{\varphi}$ is given by the expression:

$$\hat{\boldsymbol{\varphi}}_{BLUE} = (\mathbf{D}^T \mathbf{C}_{\boldsymbol{\varepsilon}}^{-1} \mathbf{D})^{-1} \mathbf{D}^T \mathbf{C}_{\boldsymbol{\varepsilon}}^{-1} \boldsymbol{\tau}. \quad (25)$$

The theorem also determines the error covariance matrix to be

$$\mathbf{C}_{BLUE} = (\mathbf{D}^T \mathbf{C}_\epsilon^{-1} \mathbf{D})^{-1}. \quad (26)$$

Using the time error covariance matrix \mathbf{C}_ϵ and the linear transformation matrix \mathbf{D} in (21), the following estimate for the target localization is obtained:

$$\hat{\mathbf{x}}_{BLUE} = [\hat{\varphi}_{BLUE}]_{2 \times 1} = -c \frac{\mathbf{G}_{BLUE}}{u_{BLUE}} \begin{bmatrix} \text{sum}(A_{lk}^c \tau_{lk}) \\ \text{sum}(B_{lk}^c \tau_{lk}) \end{bmatrix}, \quad (27)$$

where A_{lk}^c , B_{lk}^c , were defined previously, and τ_{lk} are the time observations. The elements of matrix $[\mathbf{G}_{BLUE}]_{2 \times 2}$ are expressed as :

$$[\mathbf{G}_{BLUE}]_{1,1} = \text{sum}((B_{lk}^c)^2) - \frac{1}{MN} (\text{sum}(B_{lk}^c))^2, \quad (28)$$

$$[\mathbf{G}_{BLUE}]_{2,2} = \text{sum}((A_{lk}^c)^2) - \frac{1}{MN} (\text{sum}(A_{lk}^c))^2,$$

$$[\mathbf{G}_{BLUE}]_{1,2} = [\mathbf{G}_{BLUE}]_{2,1} = \frac{1}{MN} (\text{sum}(A_{lk}^c) \text{sum}(B_{lk}^c)) - \text{sum}(A_{lk}^c B_{lk}^c),$$

and the term u_{BLUE} is defined by

$$u_{BLUE} = [\mathbf{G}_{BLUE}]_{1,1} \cdot [\mathbf{G}_{BLUE}]_{2,2} - ([\mathbf{G}_{BLUE}]_{1,2})^2. \quad (29)$$

Using these results in (26) provides the MSE for the BLUE estimates as follows:

$$\sigma_x^2(BLUE) = \frac{c^2}{8\pi^2 \text{SNR} f_c^2 f_R} \cdot \frac{[\mathbf{G}_{BLUE}]_{1,1}}{u_{BLUE}} \quad (30)$$

and for the y axis is

$$\sigma_y^2(BLUE) = \frac{c^2}{8\pi^2 \text{SNR} f_c^2 f_R} \cdot \frac{[\mathbf{G}_{BLUE}]_{2,2}}{u_{BLUE}} \quad (31)$$

The BLUE estimator in (27) provides an explicit expressions for the localization estimation. The terms A_{lk}^c and B_{lk}^c relate to the geometric layout of the transmitting and receiving radars. From the above terms one can not intuitively identify the relation between the radars positions and the obtainable accuracy. This evaluation is undertaken in the next section.

V. GDOP

The GDOP metric is commonly used in GPS for mapping the attainable localization precision for a given layout of GPS satellites positions [22], [23]. Here, we seek a metric that expresses the effect of the positions of the transmitting and receiving elements of the MIMO radar on the relationship between the time delay estimation errors and the localization errors. Plots of GDOP provide a clear view of high accuracy areas for a given set of radar locations.

The GDOP metric for the two dimensional case is defined as:

$$\text{GDOP} = \frac{\sqrt{\sigma_x^2 + \sigma_y^2}}{c\sigma_\epsilon}, \quad (32)$$

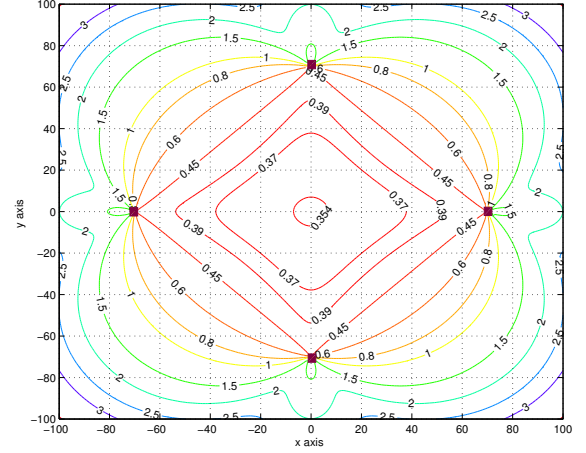


Fig. 1. GDOP contours for a symmetric positioning of radars around the axis origin: case (a) for $M=N=6$.

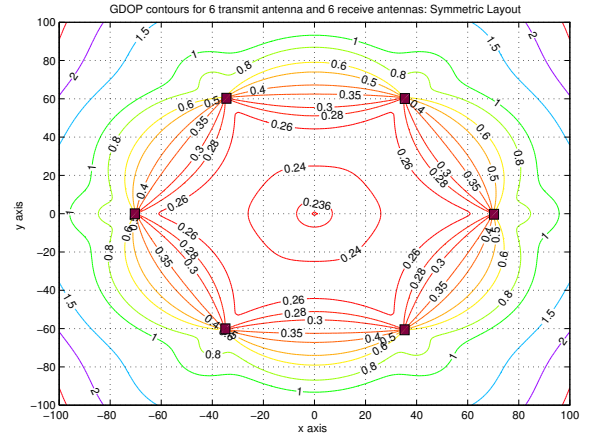


Fig. 2. GDOP contours for a symmetric positioning of radars around the axis origin: case (b) for $M=N=6$.

where σ_x^2 and σ_y^2 are the variances of localization on the x and y axis, respectively, and σ_ϵ is the standard deviation of the time delays, assumed the same for all sensors. Substituting σ_x^2 and σ_y^2 by the BLUE MSE given in (30) and (31), and using the time delay variance in (24), we get the following GDOP expression:

$$\text{GDOP}_{BLUE} = \sqrt{\frac{[\mathbf{G}_{BLUE}]_{1,1} + [\mathbf{G}_{BLUE}]_{2,2}}{u_{BLUE}}}. \quad (33)$$

In this expression, the sensors' locations are embedded in the terms A_{lk} and B_{lk} . The GDOP reduces the combined effect of the locations to a single metric. Once we get the values mapped, the actual localization error is easily derived by multiplying the GDOP value with $c\sigma_\epsilon$.

In Figures 1 and 2, contour plots of the GDOP values are presented for the case of respectively, $M = N = 4$ and $M = N = 6$ radars positioned symmetrically on the N vertices of a polygon centered at the origin. The radars are all transmitting orthogonal signals and perform time delay

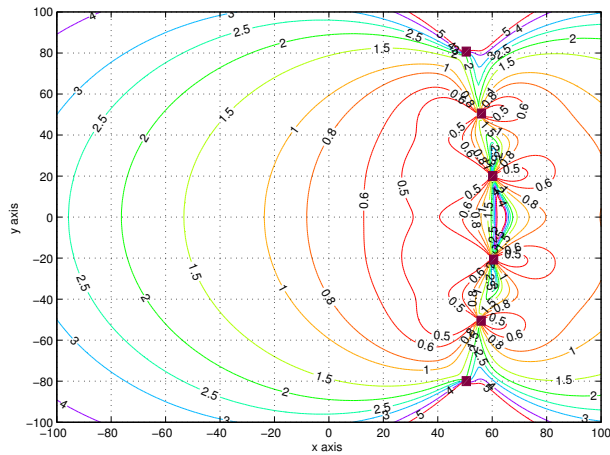


Fig. 3. GDOP contours for an asymmetric positioning of $N = M = 6$ radars, where the radar are almost aligned.

estimations. The first noticeable factor in the comparison of the two plots is the higher accuracy obtained with six radars compared to four radars. For example, the lowest GDOP value for the case of four radars is 0.354, while with six radars, the GDOP is 0.236, corresponding to a 67% improvement. All the targets located inside the virtual N-sided polygon achieve relative high accuracy localization, while the most accurate localization is obtained for the target at the center. The increase in GDOP values from the center to the polygon boundaries is slow. Outside this polygon, the GDOP values increase rather rapidly.

In Figure 3 contours of six non-symmetrically positioned radars are drawn. When the radars are not spread around the target there is a degradation in areas with good measurement accuracy. These examples show that a symmetrical deployment of sensors around the target yield lower GDOP values. Plots of GDOP provide a clear view of high accuracy areas for a given set of radar locations. These plots could also serve as a tool for choosing favorable radar locations to cover a given target area.

VI. CONCLUSIONS

The MIMO radar architecture with coherent processing exploits knowledge of the phase differences measured at the receive antennas to produce a high accuracy target location estimate. We showed that by exploiting the spatial dimension, MIMO radar with widely separated antennas may overcome bandwidth limitations and support high accuracy target localization. At the same time, this type of MIMO radar has the challenge of time and/or phase synchronizing multisite systems, and needs to deal with ambiguities stemming from the large separation between sensors. GDOP contours, mapping the relative performance accuracy for a given layout of radars over a given geographic area, were introduced. These plots offer a clear understanding of the collaboration effect of different sensor scheme on the resulting accuracy.

REFERENCES

- [1] D. R. Fuhrman, and G. San Antonio, "Transmit beam-forming for MIMO radar systems using partial signal correlation," in *Proc. of 38th ASILOMAR 2004 Conf. on Signals, Systems and Computers*, Nov. 2004, pp. 295–299.
- [2] J. Li and P. Stoica, "MIMO Radar with Colocated Antennas: Review of Some Recent Work," *IEEE Signal Processing Magazine*, Vol. 24, No. 5, pp. 106–114, September 2007.
- [3] D. W. Bliss, and K. W. Forsythe, "Multiple-input multiple-output (MIMO) radar and imaging: degrees of freedom and resolution," in *Proc. of 37th ASILOMAR 2003 Conf. on Signals, Systems and Computers*, Nov. 2003, pp. 54–59.
- [4] D. Rabideau, "Ubiquitous MIMO digital array radar," in *Proc. of 37th ASILOMAR 2003 Conf. on Signals, Systems and Computers*, Nov. 2003, pp. 1057–1064.
- [5] F. C. Robey, S. Coumts, D. Weikle, J. C. McHarg, and K. Cuomo, "MIMO radar theory and experimental results," in *Proc. of 37th ASILOMAR 2004 Conf. on Signals, Systems and Computers*, Nov. 2004, pp. 300–304.
- [6] I. Bekkerman and J. Tabrikian, "Target detection and localization using MIMO radars and sonars," *IEEE Trans. on Sig. Proc.*, vol. 54, pp. 3873–3883, Oct. 2006.
- [7] L. Xu, J. Li, and P. Stoica, "Adaptive techniques for MIMO radar," in *14th IEEE Workshop on Sensor Array and Multi-channel Processing*, Waltham, MA, July 2006.
- [8] E. Fishler, A. M. Haimovich, R. S. Blum, L. Cimini, D. Chizhik, and R. Valenzuela, "Spatial diversity in radars – models and detection performance," *IEEE Trans. on Sig. Proc.*, vol. 54, pp. 823–838, March 2006.
- [9] N. Lehmann, A. M. Haimovich, R. S. Blum, and L. Cimini, "MIMO – radar application to moving target detection in homogenous clutter," in *14th IEEE Workshop on Sensor Array and Multi-channel Processing*, Waltham, MA, July 2006.
- [10] N. Lehmann, A. M. Haimovich, R. S. Blum, and L. Cimini, "High resolution capabilities of MIMO radar," in *Proc. of 40th ASILOMAR 2006 Conf. on Signals, Systems and Computers*, Nov. 2006.
- [11] A. S. Fletcher, and F. C. Robey, "Performance bounds for adaptive coherence of sparse array radar," in *Proc. of the 11th Conf. on Adaptive on Sensor Array and Multi-channel Processing*, March 2003.
- [12] E. Fishler, A. M. Haimovich, R. S. Blum, L. Cimini, D. Chizhik, and R. Valenzuela, "MIMO radar: an idea whose time has come," in *Proc. of the 2004 IEEE Int. Conf. on Radar*, April 2004, pp. 71–78.
- [13] G. J. Foschini, "Layered space-time architecture for wireless communication in a fading environment when using multiple antennas," *Bell Labs Technical Journal*, vol. 1, No. 2, pp. 41–59, 1996.
- [14] A. M. Haimovich, R. S. Blum, and L. Cimini, "MIMO radar with Widely Separated Antennas: Reviewing Recent Work," *IEEE Signal Processing Magazine*, January 2008, pp. 116–129.
- [15] H. Godrich, A. M. Haimovich, and R. S. Blum, "Concepts And Applications Of MIMO Radar System With Widely Separated Antenna," Book Chapter, in preparation, 2007.
- [16] M. Skolnik, *Introduction to Radar Systems*. New York: McGraw-Hill, 3rd, 2002.
- [17] E. Fishler, A. M. Haimovich, R. S. Blum, L. Cimini, D. Chizhik, and R. Valenzuela, "MIMO radar: an idea whose time has come," in *Proc. of the 2004 IEEE Int. Conf. on Radar*, April 2004, pp. 71–78.
- [18] N. Levanon, *Radar Principles*. New York: John Wiley and Sons Inc., 1st ed., 1988.
- [19] S. M. Kay, *Fundamentals of Statistical Signal Processing: Estimation Theory*, vol. 1, New Jersey: Prentice Hall PTR, 1st ed., 1993.
- [20] H. Godrich, A. M. Haimovich, and R. S. Blum, "Cramer Rao Bound on Target Localization Estimation in MIMO Radar Systems", to appear in *CISS*, March 2008.
- [21] H. Godrich, A. M. Haimovich, and R. S. Blum, "Target localization accuracy gain in MIMO radar based system," to be submitted to *IEEE Trans. on Sig. Proc.*
- [22] H. B. Lee, "A novel procedure for assessing the accuracy of the hyperbolic multilateration systems," *IEEE Trans. on Aerospace and Electronic Systems*, vol. 11, pp. 2–15, Jan. 1975.
- [23] N. Levanon, "Lowest GDOP in 2-D scenarios," *IEE Proc. –Radar, Sonar, Navig.*, vol. 147, pp. 149–155, June 2000.